

Chirality tubes along monopole trajectories *

Harald Markum, Wolfgang Sakuler and Stefan Thurner

Institut für Kernphysik, TU Wien, Wiedner Hauptstraße 8-10, A-1040 Vienna, Austria

We classify the lattice by elementary 3-cubes which are associated to dual links occupied by, or free of monopoles. We then compute the quark condensate, the quark charge and the chiral density on those cubes. By looking at distributions we demonstrate that monopole trajectories carry considerably more chirality with respect to the free vacuum.

During the last years one has gained some insight into the mutual interrelations of two distinct excitations of the QCD vacuum: monopoles and instantons. Both of those objects have been used to explain a wide variety of basic QCD properties, such as quark confinement, chiral symmetry breaking [1] and the $U_A(1)$ problem. The first property is usually associated with monopoles, the later ones with instantons. Instantons have integer topological charge Q which is related to the chiral zero eigenvalues of the fermionic matrix with a gauge field configuration via the Atiyah-Singer index theorem. Since instantons carry chirality, and on the other hand it has been demonstrated that instantons are predominantly localized at regions where monopoles exist, the question arises whether monopoles carry chirality themselves. For calorons it has been proven that they consist of monopoles [2] which might be a sign that monopoles are indeed carriers of chirality.

In this contribution we discuss this issue by directly looking at the chirality located on monopole loops, and comparing it to the background. We do this by measuring conditional probability distributions of fermionic observables of the form $\bar{\psi}\Gamma\psi$ with $\Gamma = 1, \gamma_4, \gamma_5$ in a standard staggered fermion setting. Those quantities are usually referred to as the quark condensate, quark charge density, and the chiral density. Mathematically and numerically the local quark condensate $\bar{\psi}\psi(x)$ is a diagonal element of the inverse of the fermionic matrix of the QCD action. The other

fermionic operators are obtained by inserting the Euclidian γ_4 and γ_5 matrices.

Under a conditional probability distribution we understand the probability of encountering a certain value for a fermionic observable $\bar{\psi}\Gamma\psi$, under the condition that the local position is close to (or away from) a monopole trajectory,

$$P_{s/t}^{(\text{no})\text{mon}}(\bar{\psi}\Gamma\psi, x)|_{x \in (\not\in)\text{monopole tube}}, \quad (1)$$

where x is indicating the local position, and s/t space- or time-like monopole trajectories. The core of the monopole tube is the singular monopole trajectory, living on dual links, as obtained by the standard definition of monopoles in $SU(3)$. We did not distinguish between the two independent colors of monopoles. For each dual link occupied by a monopole trajectory there exists an elementary 3-cube. The 8 sites of such a cube constitute the section of the monopole tube corresponding to that dual link.

Our simulations were performed for full $SU(3)$ QCD on an $8^3 \times 4$ lattice with periodic boundary conditions. Dynamical quarks in Kogut-Susskind discretization with $n_f = 3$ flavors of degenerate mass $m = 0.1$ were taken into account using the pseudofermionic method. We performed runs in the confinement phase at $\beta = 5.2$. Measurements were taken on 2000 configurations separated by 50 sweeps.

We computed correlation functions between two observables $\mathcal{O}_1(x)$ and $\mathcal{O}_2(y)$ [3],

$$g(y-x) = \langle \mathcal{O}_1(x)\mathcal{O}_2(y) \rangle - \langle \mathcal{O}_1 \rangle \langle \mathcal{O}_2 \rangle. \quad (2)$$

In Fig. 1 we display results for \mathcal{O}_1 a local fermionic observable (except in (d)) and \mathcal{O}_2 the

*Supported in part by FWF under Contract No. P11456

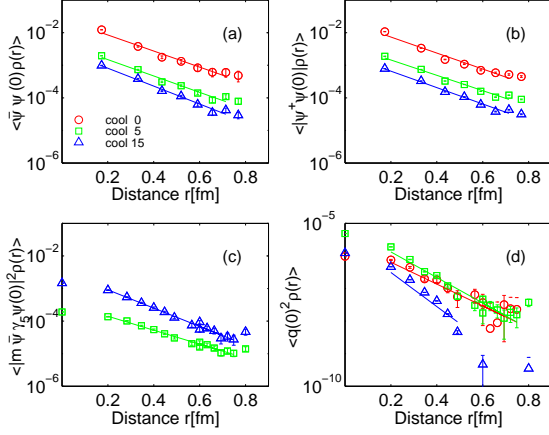


Figure 1. Correlation functions with the monopole density $\rho(r)$.

monopole charge density ρ . All correlations exhibit an extension of several lattice spacings and show an exponential falloff over the whole range. The corresponding screening masses are given in Table 1 in GeV for 3 levels of cooling. They are a coarse measure for the chirality profile of the monopole tube. It is apparent that cooling does not change the screening masses drastically.

For reasons of comparison we included in the table the screening masses for the correlation with the topological charge density (squared). We find that the correlations of the color charge density $\bar{\psi}\psi(x)$ and $|\psi^\dagger\psi(x)|$ with the topological charge density are very similar, both in the slopes and the absolute values. This becomes clear because the quark condensate can be interpreted as the absolute value of the quark density. However, cooling (or some other kind of smoothing) is inevitable to obtain nontrivial correlations between the chiral density, $\mathcal{O}_1 = \bar{\psi}\gamma_5\psi(x)$, and the topological charge density. This can be expected since both quantities are connected via the anomaly. The topological charge of a gauge field is related to the chiral density of the associated fermion field by $Q = \int q(x)d^4x = m \int \bar{\psi}\gamma_5\psi(x)d^4x$. We have checked that this relation also holds approximately for the corresponding lattice observables on individual configurations. The autocor-

Table 1

Screening masses in GeV from fits to exponential decays of the various correlators for several cooling steps.

| Correlation | cool 0 | cool 5 | cool 15 |
|--|----------|----------|----------|
| $ \psi^\dagger\psi(0) \rho(r)$ | 1.13(02) | 1.08(01) | 1.16(01) |
| $\bar{\psi}\psi(0)\rho(r)$ | 1.14(10) | 1.16(05) | 1.27(06) |
| $ \bar{\psi}\gamma_5\psi(0) ^2\rho(r)$ | - | 0.98(07) | 1.30(10) |
| $q^2(0)\rho(r)$ | 1.54(47) | 1.81(20) | 2.41(58) |
| $ \psi^\dagger\psi(0) q^2(r)$ | 1.25(66) | 1.29(10) | 1.42(09) |
| $\bar{\psi}\psi(0)q^2(r)$ | 1.32(34) | 1.38(16) | 1.47(16) |
| $\bar{\psi}\gamma_5\psi(0)q(r)$ | - | 0.84(02) | 0.48(01) |
| $q(0)q(r)$ | - | 1.67(02) | 0.84(01) |

relation function of the density of the topological charge $\langle q(0)q(r) \rangle$ should be compared to $\langle \bar{\psi}\gamma_5\psi(0)q(r) \rangle$. If the classical t'Hooft instanton with size ρ_I is considered, the topological charge density is

$$q(x) \propto \rho_I^4 (x^2 + \rho_I^2)^{-4} . \quad (3)$$

On the other hand the corresponding density of fermionic quantities [1]

$$\bar{\psi}\psi(x) \propto \bar{\psi}\gamma_5\psi(x) \propto \rho_I^2 (x^2 + \rho_I^2)^{-3} \quad (4)$$

is broader. This behavior is reflected in Table 1 and means that the local relation $q(x) = m\bar{\psi}\gamma_5\psi(x)$ does not hold.

Figure 2 shows results for the conditional probability distributions for $\bar{\psi}\psi$ (in multiples of the quark mass) in the case of monopole presence ($m=1$) or absence ($m=0$). The $m=0$ case exhibits a relatively narrow distribution of the fermionic quantity around 0.41 with a variance of 0.179 or 0.171, for space- and time-like monopole trajectories respectively. The $m=1$ case is clearly different and shows a much broader distribution, with both the mean and the variance being about a factor two larger. The time-like trajectories yield distributions which are still peaked on the left, like in the $m=0$ case, whereas this is not observed for space-like trajectories.

The plot suggests that in the close neighborhood of a monopole it becomes more likely to encounter large values of $\bar{\psi}\psi(x)$. The form of the distributions points towards a picture where

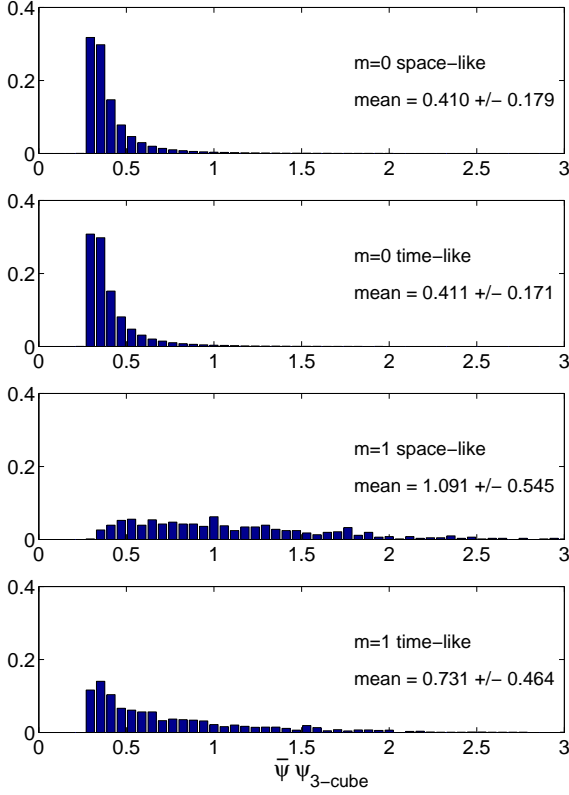


Figure 2. Conditional probability distributions for $\bar{\psi}\psi(x)$ due to monopole appearance.

monopole tubes carry a space-time dependent density of the fermionic observables. In the confinement, space-like tubes bear more chirality. The same situation is found for the other observables $\text{Re}(\psi^\dagger\psi)$ and $|\bar{\psi}\gamma_5\psi|$ (see Fig. 3). The figures depict the situation after 15 cooling steps. We checked that these observations can be made also after 5 cooling steps.

In summary, the computations of correlation functions between the monopole charge density and the fermionic observables yield an exponential decrease. The screening masses correspond to those of correlators between the topological charge density and the same fermionic observables [3]. Our calculations of conditional distribu-

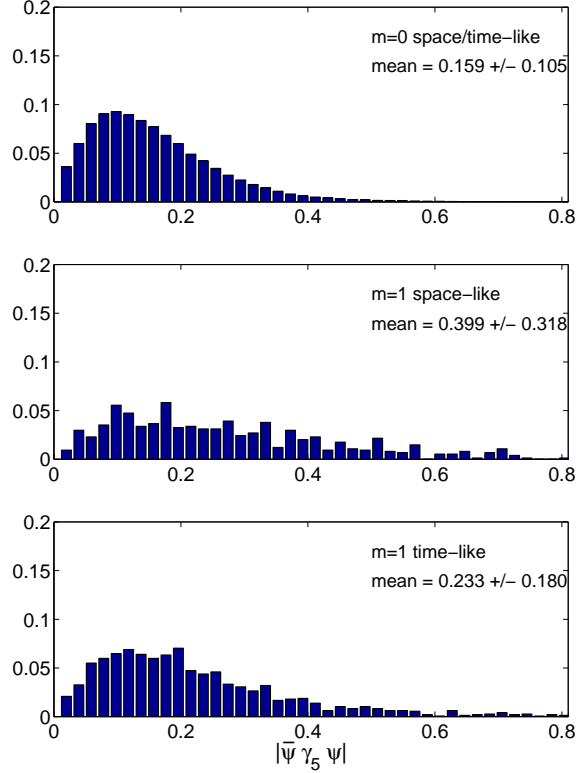


Figure 3. Conditional probability distributions for $|\bar{\psi}\gamma_5\psi(x)|$ due to monopole appearance.

tion functions of fermionic observables point out a significant enhancement for finding large chirality in the neighborhood of monopole trajectories. The same distributions also indicate that the monopoles are not covered by a uniform chirality tube.

REFERENCES

1. E.V. Shuryak, Nucl. Phys. B302 (1988) 559; T. Schäfer and E.V. Shuryak, Rev. Mod. Phys. 70 (1998) 323.
2. T.C. Kraan and P. van Baal, Nucl. Phys. B (Proc. Suppl.) 73 (1999) 554.
3. H. Markum, W. Sakuler and S. Thurner, Nucl. Phys. B (Proc. Suppl.) 73 (1999) 509.